



## Assessment of Wind Turbine Driven DFIG Using AC/DC/AC Converter

**Preeti Singh**

*M.Tech. Research Scholar  
Takshshila Institute of Engineering & Technology  
Jabalpur, (M.P.) [INDIA]  
Email: [preeti151995@gmail.com](mailto:preeti151995@gmail.com)*

**Pramod Dubey**

*Assistant Professor  
Department of Electrical & Electronics Engineering.  
Takshshila Institute of Engineering & Technology  
Jabalpur (M.P.), [INDIA]  
Email: [pramoddubey@takshshila.org](mailto:pramoddubey@takshshila.org)*

### ABSTRACT

*The evolution of technology related to wind systems industry led to the development of a generation of variable speed wind turbines that present many advantages compared to the fixed speed wind turbines. These wind energy conversion systems are connected to the grid through Voltage Source Converters (VSC) to make variable speed operation possible. The studied system here is a variable speed wind generation system based on Doubly Fed Induction Generator (DFIG). To harness the wind power efficiently the most reliable system in the present era is grid connected doubly fed induction generator. The rotor side converter (RSC) usually provides active and reactive power control of the machine while the grid-side converter (GSC) keeps the voltage of the DC-link constant.*

**Keywords:**—Grid-side converter (GSC), rotor side converter (RSC) Doubly Fed Induction Generator (DFIG), squirrel cage induction generators (asynchronous generators) .

### I. INTRODUCTION

With increased penetration of wind power into electrical grids, DFIG wind turbines are largely deployed due to their variable speed feature and hence influencing system dynamics. This has created an interest in developing suitable models for DFIG to be

integrated into power system studies. The continuous trend of having high penetration of wind power, in recent years, has made it necessary to introduce new practices. For example, grid codes are being revised to ensure that wind turbines would contribute to the control of voltage and frequency and also to stay connected to the host network following a disturbance.

As shown in figure 1, the squirrel cage induction generators (asynchronous generators) are directly connected to the grid through a step up power transformer. These types of the generators are also known as a constant or fixed speed wind generators because they are operated with less than 1% variation of rotor speed. Moreover, the squirrel cage induction generators always consume reactive power. Therefore, the capacitor bank connected close to the generators to compensate the reactive power consumption in order to achieve a unity power factor. Thus, these generators are undesirable in the large wind turbines due to their limitation in power capture.

For full converter induction machine as shown in figure 2, the induction machine is connected to the grid directly through fully rated power converters and a power transformer.

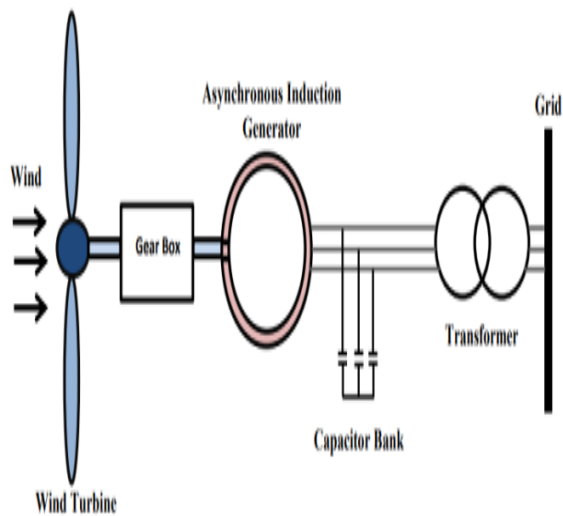


Figure 1. A fixed speed asynchronous wind generator.

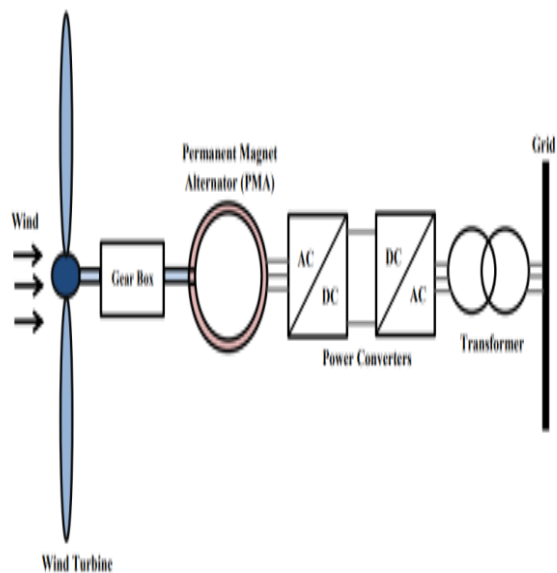


Figure 2: Induction machine with full converter interface.

## II. BACK TO BACK AC/DC/AC CONVERTER

### Modeling

A back-to-back converter is needed for a control of a doubly-fed induction machine (an induction machine fed from both the rotor and the stator) because in some operation ranges the rotor energy may come back to the converter [1]. A back-to-back converter has the feature that the power can flow to any direction. Figure 3 shows a

back-to-back converter made of a full bridge AC/DC monophasic boost-like rectifier and a 3-phase DC/AC inverter. Mathematical modeling of converter system is realized by using various types of models, which can be broadly divided into two groups: mathematical functional models and Mathematical physical models (either equation-oriented or graphic-oriented, where graphic-oriented approach is actually based on the same differential equations).

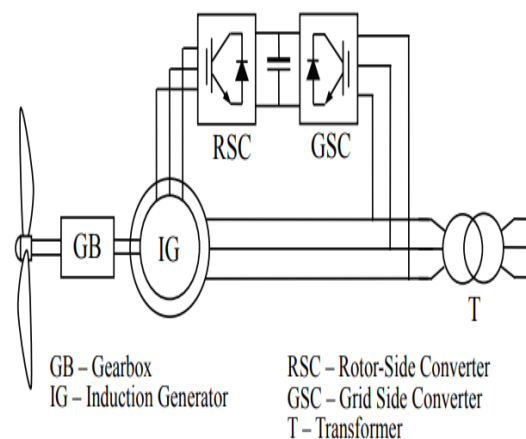


Figure 3: Typical back-to-back arrangement of inverter and converter circuits to control power flow.

At the current state of development, most DFIG power electronics utilise a two-level six switch converter, Figure 4 Two-level refers to the number of voltage levels that can be produced at the output of each bridge leg of the converter. A two-level converter can typically output zero volts or  $V_{dc}$ , where  $V_{dc}$  is the voltage of the dc link. Figure 3 shows two such converters connected in a back-to-back arrangement with a DC link between the two converters. The switching elements in higher power converters are likely to be Insulated gate Bipolar Transistors (IGBTs). The six-switch converter can synthesise a three-phase output voltage which can be of arbitrary magnitude, frequency and phase, within the constraint that the peak line voltage is less than the DC link voltage.

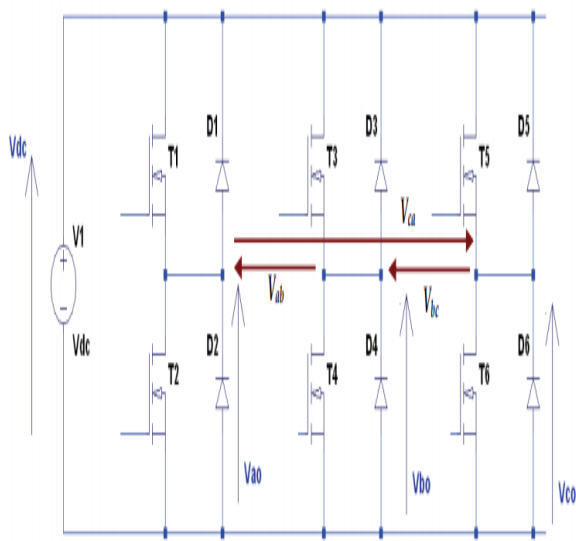


Figure 4. Six-switch voltage source inverter circuit.

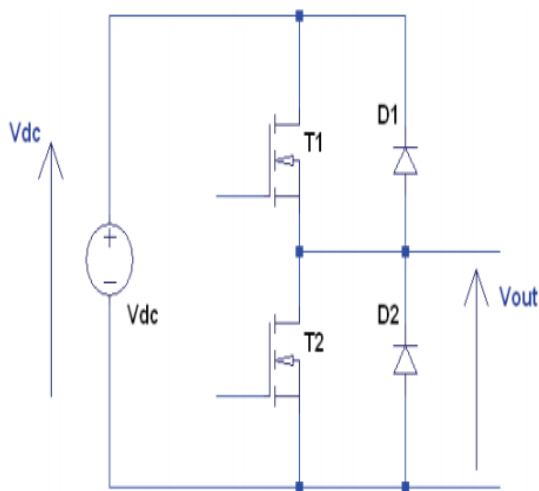


Figure 5. One bridge leg of a voltage source inverter circuit.

The average output voltage, at the terminals of the bridge leg,  $V_{out}$ , is given by

$$V_{out} = V_{dc} \frac{t_{1on}}{t_{sw}}$$

Where  $T_{sw}$  is the switching period, and  $t_{1,on}$  is the on time of the switch T1. We define the duty cycle, or modulation index,  $m$  as

$$\frac{t_{1on}}{t_{sw}}$$

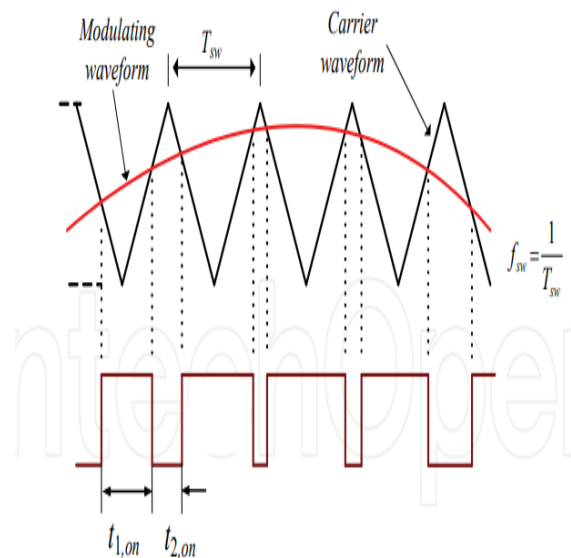


Figure 6: Example of carrier-based pulse-width modulated signal generation.

Hence  $V_{out} = mV_{dc}$

where  $m$  must be between 0 (T2 on continuously) and 1 (T1 on continuously). The modulation index,  $m$ , can be varied in time, therefore any desired voltage and frequency can be generated at the output terminals (within the bounds fixed by the switching frequency and  $V_{dc}$ ). In the three-phase converter shown in Figure 5, there are three phase legs, hence three modulation indices,  $m_a$ ,  $m_b$  and  $m_c$ . The voltages between the mid-point of each phase leg and the 0V node of the dc link are

$$\begin{cases} V_{a0} = m_a V_{dc} \\ V_{b0} = m_b V_{dc} \\ V_{c0} = m_c V_{dc} \end{cases}$$

Now if each modulation index varies sinusoidally according to

$$\begin{cases} m_a = \frac{1}{2} + m \sin(\omega t) \\ m_b = \frac{1}{2} + m \sin\left(\omega t - \frac{2\pi}{3}\right) \\ m_c = \frac{1}{2} + m \sin\left(\omega t + \frac{2\pi}{3}\right) \end{cases}$$

Then the resultant output line voltages will take the form

$$\begin{cases} V_{ab} = V_{a0} - V_{b0} = \sqrt{3m} V_{dc} \sin\left(\omega t - \frac{\pi}{6}\right) \\ V_{bc} = V_{b0} - V_{c0} = \sqrt{3m} V_{dc} \sin\left(\omega t - \frac{5\pi}{6}\right) \\ V_{ca} = V_{c0} - V_{a0} = \sqrt{3m} V_{dc} \sin\left(\omega t + \frac{\pi}{2}\right) \end{cases}$$

In steady-state at fixed turbine speed for a lossless DFIG system, the mechanical power from the wind turbine applied to the shaft is  $P_m = P_s + P_r$ . It follows that:

$$P_r = P_m - P_s = T_m \omega_r - T_{em} \omega_s = -T_m \left( \frac{\omega_s - \omega_r}{\omega_s} \right) \omega_s = -s T_m \omega_s = -s P_s$$

where  $s$  is defined as the slip of the generator:

$$s = \left( \frac{\omega_s - \omega_r}{\omega_s} \right)$$

Therefore if the maximum slip is limited, say to 0.3, the rotor winding converters can be rated as a fraction of the induction generator rated power.

$$P_m = C_{p-pu} V_{wind-pu}^3$$

**DC-link model** The dc-link model describes the dc-link capacitor voltage variations as a function of the input power to the dc-link (Ledesma & Usaola, 2005). The energy stored in the dc capacitor is

$$W_{dc} = \int P_{dc} dt = \frac{1}{2} C V_{dc}^2$$

Where  $C$  is the capacitance,  $V_{dc}$  is the voltage,  $W_{dc}$  is the stored energy, and  $P_{dc}$  is the input power to the dc link. The voltage and energy derivatives are

$$\frac{dV_{dc}}{dt} = \frac{P_{dc}}{C V_{dc}}, \quad \frac{dW_{dc}}{dt} = P_{dc}$$

The  $P_{dc}$  is calculated as  $P_{dc} = P_{in} - P_c$ . Where  $P_{in}$  is the input power from rotor-side converter and  $P_c$  is the grid-side converter output power. The steady-state equations governing the real and reactive power flow from the grid-side converter to the grid are

$$P = \frac{VE \sin \delta}{X_s} \quad \text{and} \quad Q = \frac{V^2}{X_s} - \frac{VE}{X_s} \cos \delta$$

where  $X_s$  is the reactance of the interfacing inductance. If  $\delta$  is small the equations can be simplified to

$$P = \frac{VE \delta}{X_s} \quad \text{and} \quad Q = \frac{V^2}{X_s} - \frac{VE}{X_s}$$

Showing that  $P$  can be controlled using load angle,  $\delta$ , and  $Q$  can be controlled using the magnitude of  $E$ .

### III. RESULT AND CONCLUSION

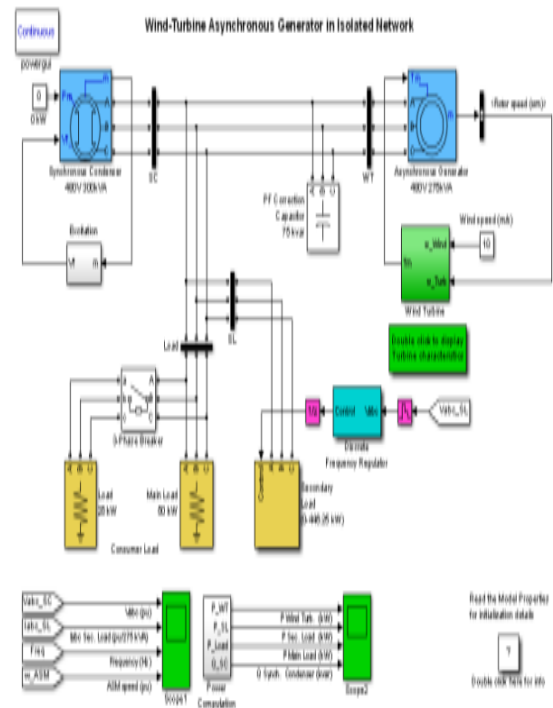


Figure 7 : Wind turbine driven Isolated Induction Generator model Simulation in SIMULINK

#### Output Characteristics

Turbine response to a change in wind speed We Started simulation and observed the signals on the “Wind Turbines” scope monitoring active and reactive power, generator speed, wind speed and pitch angle for each turbine.

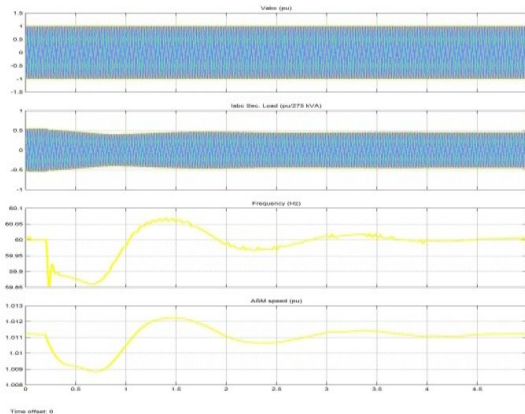


Figure 8: Voltage and Current Characteristic

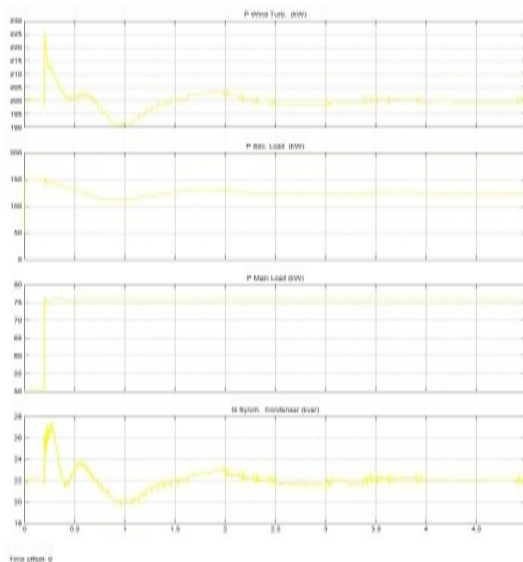


Figure 9: Active Power of Wind Turbine, Loads and Reactive Power of Synchronous Condenser

For each pair of turbine the generated active power starts increasing smoothly (together with the wind speed) to reach its rated value of 3 MW in approximately 8s. Over that time frame the turbine speed will have increased from 1.0028 pu to 1.0047 pu. Initially, the pitch angle of the turbine blades is zero degree. When the output power exceed 3 MW, the pitch angle is increased from 0 deg to 8 deg in order to bring output power back to its nominal value. Observe that the absorbed reactive power increases as the generated active power increases. At nominal power, each pair of wind turbine absorbs 1.47 Mvar.

For a 11m/s wind speed, the total exported power measured at the B25 bus is 9 MW and the statcom maintains voltage at 0.984 pu by generating 1.62 Mvar Conclusion

At t=15 s, a phase to phase fault is applied at wind turbine 2 terminals, causing the turbine to trip at t=15.11s. If you look inside the “Wind Turbine Protections” block you will see that the trip has been initiated by the AC Under voltage protection. After turbine 2 has tripped, turbines 1 and 3 continue to generate 3 MW each.

#### REFERENCES:

- [1] Hans Øverseth Røstøen Tore M. Undeland Terje Gjengedal' IEEE paper on doubly fed induction generator in a wind turbine.
- [2] S. K Salman and Babak Badrzadeh School of Engineering, The Robert Gordon University, IEEE paper on New Approach for modelling Doubly -Fed Induction Generator (DFIG) for grid-connection studies.
- [3] Sloopweg JG, Polinder H, Kling WL. Dynamic modeling of a wind turbine with doubly fed induction generator. IEEE Power Engineering summer meeting, 2001; Vancouver, Canada.
- [4] Holdsworth L, Wu XG, Ekanayake JB, Jenkins N. Comparison of fixed speed and doubly-fed induction wind turbines during power system disturbances. IEE Proceedings: Generation, Transmission, Distribution, 2003, 3: 343-352
- [5] Ekanayake, J.B, Holdsworth, L, Wu, X., Jenkins, N. Dynamic modeling of Doubly Fed Induction generator wind turbines. IEEE Transaction on Power Systems, 2003, 2:803-809

- [6] J. Morren, J.T.G. Pierik, S.W.H. de Haan, J. Bozelie, “Grid interaction of offshore wind farms. Part 1. Models for dynamic simulation”, *Wind Energy*, 8 (3): JUL-SEP 2005.
  
- [7] R. Pena, J.C. Clare, G.M. Asher, “Doubly-fed induction generator using back-to-back PWM converters and its applications to variable-speed wind-energy generation”, *IEEE Proceedings on Electrical Power Applications*, Vol. 143, No. 3, May 1996, pp. 231-341.
  
- [8] The Math Works, “SimPowerSystems For Use with Simulink”, User’s Guide Version
  
- [9] Richard Gagnon, Gilbert Sybille, Serge Bernard, Daniel Paré, Silvano Casoria, Christian Larose “Modeling and Real-Time Simulation of a Doubly-Fed Induction Generator Driven by a Wind Turbine” Presented at the International Conference on Power Systems Transients (IPST’05) in Montreal, Canada on June 19-23, 2005 Paper No. IPST05-162.

\* \* \* \* \*